

## **Optical Properties of Ice Particles in Young Contrails**

**Gang Hong, Qian Feng, Ping Yang, George Kattawar**

Texas A&M University

College Station, TX 77843, USA

**Patrick Minnis and Yong X. Hu**

NASA Langley Research Center, Hampton, VA 23681

For publication in

*Journal of Quantitative Spectroscopy and Radiative Transfer*

---

*Corresponding author address:* Dr. Gang Hong, Department of Atmospheric Sciences,  
Texas A&M University, College Station, TX 77843; Tel: 979-845-5008.

Email: [hong@ariel.met.tamu.edu](mailto:hong@ariel.met.tamu.edu)

## **Abstract**

The single-scattering properties of four types of ice crystals (pure ice crystals, ice crystals with an internal mixture of ice and black carbon, ice crystals coated with black carbon, and soot coated with ice) in young contrails are investigated at wavelengths 0.65 and 2.13  $\mu\text{m}$  using Mie codes from coated spheres. The four types of ice crystals have distinct differences in their single-scattering properties because of the embedded black carbon. The bulk scattering properties of young contrails consisting of the four types of ice crystals are further investigated by averaging their single-scattering properties over a typical ice particle size distribution found in young contrails. The effect of the radiative properties of the four types of ice particles on the Stokes parameters  $I$ ,  $Q$ ,  $U$ , and  $V$  is also investigated for different viewing zenith angles and relative azimuth angles with a solar zenith angle of  $30^\circ$  using a vector radiative transfer model based on the adding-doubling technique. The Stokes parameters at a wavelength of 0.65  $\mu\text{m}$  show pronounced differences for the four types of ice crystals. Those at a wavelength of 2.13  $\mu\text{m}$  show similar variations with the viewing zenith angle and relative azimuth angle, but their values are noticeably different.

## 1. Introduction

Contrails generated from high-altitude aircraft exhaust may be potentially important for climate study on both regional and global scales (IPCC, 1999; Minnis et al., 1999, 2004; Myhre and Stordal, 2001; Ponater et al., 2002; Stuber and Forster, 2007). The impact of contrails and contrail-induced cirrus on the terrestrial climate system is likely to become more prominent, as air traffic increases 2-5% annually (Minnis et al. 1999, 2004). However, the climate effects of these clouds, measured in terms of their radiative forcing, are extremely uncertain (IPCC, 1999).

Improved knowledge about the microphysical and optical properties of contrails is critical to reducing the uncertainties in the current understanding of contrail radiative forcing. The microphysical and optical properties of contrails and contrail-induced cirrus clouds are quite different from those of natural cirrus clouds (Chylek and Hallett, 1992; Gayet et al., 1996; Petzold et al., 1997; Kuhn et al., 1998; Störm and Ohlsson, 1998; Schröder et al., 2000; Kärcher et al., 2007). Unlike a natural cirrus cloud within which ice crystals have a wide size spectrum, a contrail usually has a higher number concentration of small ice crystals (Gayet et al., 1996; Minnis et al., 1998; Ström and Ohlsson, 1998; Meerkötter et al., 1999; Schröder et al., 2000; Ponater et al., 2002). During the transition of contrails into cirrus clouds, the ice crystal size increases and the corresponding number concentration decreases, as articulated by Schröder et al. (2000) who analyzed the microphysical properties of contrails and contrail-induced cirrus clouds observed during 15 airborne missions over central Europe. It is there found that contrails are dominated by high concentrations ( $> 100 \text{ cm}^{-3}$ ) of quasi-spherical ice crystals (i.e., droxtals) with mean diameters in the range of 1-10  $\mu\text{m}$ . Larger ice crystals in the range 10-20  $\mu\text{m}$  with typical

concentrations  $2\text{-}5\text{ cm}^{-3}$  are found in young contrail-cirrus clouds that consist mostly of regularly shaped ice crystals.

Contrail particles have been found to contain soot, i.e., black carbon (Chylek and Hallett, 1992; Petzold et al., 1997; Kuhn et al., 1998; Störm and Ohlsson, 1998). The scattering and radiative properties of soot have been extensively studied (e.g., Chylek et al., 1995; Clarke et al., 2004; Mishchenko et al., 2004; Mackowski, 2006; Liu and Mishchenko, 2005, 2007) because soot plays a significant role in the absorption of solar radiation by atmospheric aerosols. The effect of black carbon on the scattering and absorption of solar radiation by cloud droplets has been investigated for almost four decades (Danielson et al., 1969; Chylek et al., 1984, 1996, 2000; Twohy et al., 1989; Macke, 2000; Liu et al., 2002). Soot, either as an external attachment or as an internal inclusion, changes the refractive index of ice particles (Chylek and Hallett, 1992; Macke et al., 1996; Kuhn et al., 1998; Yang et al., 2002), and influences the scattering properties of ice particles, thereby altering the radiative forcing of ice clouds.

The influence of soot inclusions on the visible and infrared radiative properties of ice crystals has not been extensively investigated. Macke et al. (1996) examined the influence for large ice particles at visible wavelengths. Chylek and Hallett (1992) showed that the effect of soot on the optical properties of contrail particles depends on the type of external or internal mixing and the volume fraction of soot. Kuhn et al. (1998) found a mixture of pure ice particles, black carbon aerosol, and an internal mixture of these components in the contrails using the measurements acquired during the SULFUR-4 experiment in March 1996 over southern Germany. In their findings, the volume fraction of the black carbon attached to or included within ice crystals was approximately 15-

20%. Furthermore, the contrail was found to be a mixture of 15% ice particles, 32% ice with black carbon, and 24% black carbon, and 29% unknown aerosols. These results derived for a young contrail well illustrates the importance of obtaining the accurate refractive indices of ice particles and aerosols in the contrails, and the components of ice particles and aerosols.

In the present study, the optical properties of four types of ice crystals, namely pure ice crystals, ice crystals with an internal mixture of ice and black carbon, ice crystals coated with black carbon, and soot coated with ice, are investigated at wavelengths 0.65 and 2.13  $\mu\text{m}$ . The rest of this paper is organized as follows. Section 2 presents the aforementioned four ice crystal models. Additionally, in section 2 the Mie codes for coated spheres and a vector radiative transfer model used for the present single-scattering and radiative transfer simulations are also briefly described, respectively. Section 3 presents the single-scattering properties and bulk optical properties of the contrail particles and the simulation of the Stokes parameters associated with contrails. Finally, the summary is given in section 4.

## **2. Methodology**

### ***2.1. Ice crystal models***

A large number concentration with small ice crystals is generally observed in contrails (e.g., Gayet et al., 1996; Minnis et al., 1998; Ström and Ohlsson, 1998; Meerkötter et al., 1999; Schröder et al., 2000; Ponater et al., 2002). These ice particles in contrails have been found to be quasi-spherical (Schröder et al., 2000). Additionally, the

external and internal mixtures of black carbon and ice crystals have been found in young contrails (Chylek and Hallett, 1992; Kuhn et al., 1998).

Four types of ice crystals found in young contrails used in the present study are shown in Figure 1. The pure ice particle (Figure 1a) is composed of pure ice. The particles with internal mixtures of ice and black carbon are typically represented for contrail particles (Figure 1b) and, hereafter, are denoted as contrail particles. The black carbon volume ratio was found to be 15-20% for ice particles with the internal mixture of ice and black carbon (Kuhn et al., 1998). In this study, the volume ratio of 20% is used. This volume ratio is also used for the coated soot (Figure 1c) with pure ice and the coated ice (Figure 1d) with black carbon.

The pure ice particle's refractive index is from Warren (1984). The black carbon refractive index is from the database of Levoni et al. (1997). The refractive index of a contrail particle,  $m$ , can be calculated as follows (Levoni et al., 1997):

$$m = \frac{v_i m_i + v_b m_b}{v_i + v_b}, \quad (1)$$

where  $m_i$  and  $m_b$  are the refractive indexes of pure ice and black carbon, respectively,  $v_i$  and  $v_b$  are the volume mixing ratios of pure ice and black carbon, respectively. The black carbon volume ratio is assumed to be 20% in this study. The refractive indexes of the four types of ice crystals are given in Table 1.

## ***2.2. Mie codes for coated spheres***

The conventional Lorenz-Mie formalism has been extended to study the scattering properties of coated spheres (e.g., Kattawar and Hood 1976; Toon and Ackerman, 1981; Bohren and Huffman, 1983; Kaiser and Schweiger, 1993; Fuller 1993; Mishchenko et al.

2000; Fuller and Mackowski 2000; Yang et al. 2002). In the present study, the standard code DMiLay.f for Mie calculations for coated spheres from Warren Wiscombe (NASA Goddard Space Flight Center). DMLay.f is a double precision version MieLay.f, which was based on the formulas presented in Toon and Ackerman (1981). The Mie codes for coated spheres are available at <http://atol.ucsd.edu/scatlib/codes2/wiscombe.zip>. The four types of ice crystals considered here are spherical so that the phase matrix  $\mathbf{P}(\cos\Theta)$  has only four independent matrix elements as follows (van de Hulst, 1957):

$$\mathbf{P}(\cos\Theta) = \begin{bmatrix} P_{11} & P_{12} & 0 & 0 \\ P_{12} & P_{11} & 0 & 0 \\ 0 & 0 & P_{33} & P_{34} \\ 0 & 0 & -P_{34} & P_{33} \end{bmatrix}. \quad (2)$$

### 2.3. *Vector radiative transfer model*

A number of vector radiative transfer models have been developed on the basis of different techniques, including the Monte Carlo method (Kattawar and Plass, 1968; Davis et al., 2005), the adding-doubling model (Hansen and Travis, 1974; de Haan et al., 1987; Evans and Stephens, 1991), and the vector discrete-ordinates method (Weng, 1992a, 1992b; Schulz et al., 1999), and the successive-orders-of-scattering method (Vermote et al., 1997).

In this study, the vector radiative transfer model developed by de Haan et al. (1987) on the basis of the adding-doubling method is employed to simulate the full four Stokes parameters for contrails. This vector radiative transfer model is suitable for simulating radiation at solar wavelengths. In this model, the six independent matrix elements of the phase matrix in Equation 2 are taken into account. The details of this

vector radiative transfer computational package were documented by de Haan et al. (1987).

### 3. Results

#### 3.1. Single-scattering properties

The single-scattering properties of pure ice crystals, contrail particles, coated soot with ice, and coated ice with black carbon are computed using the coated-sphere Mie code for spherical particles with diameters in the range of 0.02-4.0  $\mu\text{m}$ . Figure 2 shows the extinction efficiency  $Q_{ext}$ , absorption efficiency  $Q_{abs}$ , single-scattering albedo  $\omega$ , and asymmetry factor  $g$  as functions of  $D$  at wavelengths 0.65 and 2.13  $\mu\text{m}$  for the four types of ice crystals. The single-scattering properties of the four types of ice crystals show pronounced differences. The internal mixture of the contrail particle results in the strongest absorption efficiency followed by the ice coated with soot and the black carbon coated with ice. The absorption for all carbon-ice combinations exceeds that for pure ice, especially at 0.65  $\mu\text{m}$ . This feature is also indicated by their  $\omega$  values that tend to be in the range of 0.5-0.75, while the  $\omega$  values of pure ice crystals are 1.0 at 0.65  $\mu\text{m}$  for all sizes and at 2.13  $\mu\text{m}$  for particle diameters over 0.5  $\mu\text{m}$ .

The four nonzero phase matrix elements for the four types of ice crystals are shown in Figures 3 and 4 for 0.65 and 2.13  $\mu\text{m}$ , respectively, at a size parameter of 4. It is evident that the phase matrix elements at 2.13  $\mu\text{m}$  are essentially the same as those at 0.65  $\mu\text{m}$ . In the forward scattering directions ( $\Theta < 50^\circ$ ), the values of  $P_{11}$  for the four types of ice crystals are similar. Distinct differences are found in backward scattering directions. The elements of  $P_{12}$ ,  $P_{33}$ , and  $P_{34}$  also show pronounced differences.



### 3.2. Bulk scattering properties

Lognormal particle size distributions have been used for ice particles in contrails and aerosols (e.g., Levoni et al., 1997; Gierens and Ström, 1998), given by

$$N(D) = \frac{N_0}{D\sqrt{2\pi} \ln \sigma} \exp\left[-\frac{(\ln D - \ln D_m)^2}{2(\ln \sigma)^2}\right], \quad (3)$$

where  $N_0$  is the total number,  $D$  is the maximum dimension of the ice particle,  $D_m$  is the median particle diameter, and  $\sigma$  is the standard deviation. The single-scattering properties are computed for  $D$  ranging from 0.02 to 4.0  $\mu\text{m}$  with 200 size bins. Furthermore, we define the effective particle size  $D_e$ , following Hansen and Travis (1974), Foot (1988) and King et al. (2004),

$$D_e = \frac{\sum_{i=1}^{200} D_i^3 N(D_i) \Delta D_i}{\sum_{i=1}^{200} D_i^2 N(D_i) \Delta D_i}, \quad (4)$$

where  $i$  is the index for the size bin, and  $\Delta D$  is the bin width. Schröder et al. (2000) give several typical ice crystal number size distributions for contrails. The  $D_e$  and  $D_m$  for a fresh contrail are 1.5 and 1.2  $\mu\text{m}$ , respectively. Here we use these two values to derive the standard deviation  $\sigma$  in Equation (1), which is 1.35.

The single-scattering properties of ice particles are averaged over the log-normal particle size distribution to compute the bulk scattering properties at values  $D_e = 1.5 \mu\text{m}$ . The mean scattering efficiency  $\bar{Q}_{sca}$ , absorption efficiency  $\bar{Q}_{abs}$ , extinction efficiency  $\bar{Q}_{ext}$ , single-scattering albedo  $\bar{\omega}$ , asymmetry factor  $\bar{g}$ , and the phase matrix elements

$\bar{\mathbf{P}}(\Theta)$  are derived via the same formulas used in Yang et al. (2005) and Hong et al. (2007).

The values of  $\bar{Q}_{sca}$ ,  $\bar{Q}_{abs}$ ,  $\bar{Q}_{ext}$ ,  $\bar{\omega}$ , and  $\bar{g}$  for young contrails composed of the four types of ice crystals are listed in Table 2. Similar to the single-scattering properties shown in Figure 2, strong absorption is noticed for contrail particles, ice-coated soot, and black-carbon-coated ice though pure ice crystals are relatively non-absorptive, especially at 0.65  $\mu\text{m}$ . The values of  $\bar{g}$  are similar for pure ice crystals, contrail particles, and coated ice with black carbon for 2.13  $\mu\text{m}$ . Furthermore, these values are larger than those for coated soot with ice. The value of  $\bar{g}$  for pure ice crystals is close to that for coated soot with ice while the value of  $\bar{g}$  for contrail particles is close to that for coated ice with black carbon for 0.65  $\mu\text{m}$ .

Figure 5 shows the mean phase matrix elements ( $\bar{P}_{11}$ ,  $\bar{P}_{12}$ ,  $\bar{P}_{33}$ , and  $\bar{P}_{34}$ ) for young contrails with  $D_e = 1.5 \mu\text{m}$  at a wavelength of 0.65  $\mu\text{m}$ . The mean phase matrix elements for young contrails composed of the four types of ice crystals show significant differences. The pronounced differences are also observed in those for the wavelength 2.13  $\mu\text{m}$  shown in Figure 6.

### **3.3. Stokes parameters**

The bulk scattering properties are input to the vector radiative transfer model to simulate the Stokes parameters ( $I$ ,  $Q$ ,  $U$ ,  $V$ ) above young contrails composed of the four types of ice crystals. The incident natural sunlight is unpolarized with  $(I_0, Q_0, U_0, V_0) = (1, 0, 0, 0)$ . The incident zenith angle is set at 30°. The relative azimuth angle between the

incident and scattered radiation beams varies from 0° to 360°. The viewing zenith angle ranges from 0° to 80°. The surface is assumed to be Lambertian with an albedo of 0.1.

The optical thicknesses of contrails vary typically between 0.1 and 0.5 (e.g., Sassen, 1997; Minnis et al., 1998; Meerkötter et al., 1999; Myhre and Stordal, 2001; Ponater et al., 2002; Minnis et al., 2005; Stuber and Forster, 2007). The lowest observed value of contrail optical thickness is  $3.0 \times 10^{-5}$  (Schröder et al., 2000). Larger values of optical thickness,  $>1.0$ , were also found at higher temperatures (up to  $-30^{\circ}\text{C}$ ) (Gayet et al., 1996).

In the present study, the optical thickness of 0.3 at a visible wavelength is used for the young contrail for simulations of the Stokes parameters associated with a young contrail. The optical thickness of 0.3 at the visible wavelength is converted to that at  $2.13 \mu\text{m}$  on the basis of the following relationship:

$$\tau(2.13) = \tau(0.65) \frac{\bar{Q}_{ext}(2.13)}{\bar{Q}_{ext}(0.65)}, \quad (5)$$

where  $\tau(0.65)$  is the optical thickness of contrails at a visible ( $0.65 \mu\text{m}$ ) wavelength, i.e., 0.3 used in the present study,  $\tau(2.13)$  is the optical thickness of contrails at wavelength  $2.13 \mu\text{m}$ , and  $\bar{Q}_{ext}(0.65)$  and  $\bar{Q}_{ext}(2.13)$  are the mean extinction efficiencies (Table 2) at  $0.65$  and  $2.13 \mu\text{m}$ , respectively.

Figure 7 shows the simulated Stokes parameters associated with the contrails at wavelength  $0.65 \mu\text{m}$ . The Stokes parameters for the four types of ice crystals have distinct differences in patterns and values. The values of the Stokes parameters  $Q$ ,  $U$ , and  $V$  are smaller than those of  $I$  with an order magnitude of 1-4. Each of the Stokes

parameters for wavelength 2.13  $\mu\text{m}$  (Figure 8) have similar patterns, but slightly different values, for the four types of ice crystals.

#### **4. Summary**

The single-scattering properties of ice crystals in contrails are fundamental to understanding the radiative forcing of contrails. Four types of ice crystals, including pure ice crystals, contrail particles with an internal mixture of pure ice and black carbon, coated soot with ice, and coated ice with black carbon, have been found in young contrails. In this study, the single-scattering properties (absorption efficiency, extinction efficiency, single-scattering albedo, asymmetry factor, and scattering phase matrix) of the four types of ice crystals with maximum dimensions ranging from 0.01 to 2.0  $\mu\text{m}$  are computed from the Wiscombe Mie codes for coated spheres at wavelengths 0.65 and 2.13  $\mu\text{m}$ . The single-scattering properties of the four types of ice crystals show pronounced differences. Ice crystals including black carbon have significant absorption efficiencies in comparison with the pure ice crystals.

The single-scattering properties are averaged over a typical lognormal ice particle size distribution for a young contrail to derive the bulk scattering properties of the young contrail. Similar to the single-scattering properties, the bulk scattering properties of contrails composed of the four types of ice crystals also show pronounced differences. The embedded black carbon strongly increases the absorption of contrail particles, coated ice with black carbon, and coated soot with ice at wavelengths 0.65  $\mu\text{m}$  and 2.13  $\mu\text{m}$ .

A rigorous vector radiative transfer model developed by de Haan et al. (1987) is employed to simulate the full Stokes parameters by young contrails consisting of the four

types of ice crystals. The simulated Stokes parameters for the contrails at the wavelength 0.65  $\mu\text{m}$  distinctly vary with viewing zenith and relative azimuth angles. The variations are evident in both patterns and values. However, each of the Stokes parameters for the wavelength 2.13  $\mu\text{m}$  shows similar patterns for the four types of ice crystals although their values are slightly different.

In addition to providing the basis for improved computation of the radiative forcing by young contrails, the results of this study suggest that contrail detection from satellite imagers can be improved. Current detection methods rely on contrail linearity and small particle size. However, such signatures are not unique to contrails and result in the misidentification of many cirrus streamers as contrails (e.g., Minnis et al. 2005). Natural cirrus particles are close to being pure ice and, thus, should differ from carbon-contaminated in both polarization and spectral signatures. These signatures should be examined to determine the potential for differentiating between natural cirrus and contrails.

This study is the first step in providing a more realistic characterization of contrail optical properties. It has only considered spherical ice and ice-carbon particles for young contrails. Long-lived contrails grow rapidly in size and the particles within them also grow to various shapes and sizes. A more comprehensive treatment of the older, larger particles and the overall radiative forcing of contrails will be undertaken in future studies.

### **Acknowledgements**

Ping Yang's research is supported by the National Science Foundation Physical Meteorology Program (ATM-0239605), and a research grant (NNL06AA23G) from the

National Aeronautics and Space Administration (NASA). George Kattawar's research is supported by the Office of Naval Research under contracts N00014-02-1-0478 and N00014-06-1-0069. Patrick Minnis is supported through the NASA Modeling and Analysis Program and the NASA Clouds and the Earth's Radiant Energy System Project.

## References

- Baum, B. A., A. J. Heymsfield, P. Yang, S. T. Bedka (2005a), Bulk scattering properties for the remote sensing of ice clouds. Part I: Microphysical data and models. *J. Appl. Meteorol.*, 44, 1885–1895.
- Baum, B. A., P. Yang, A. J. Heymsfield, S. Platnick, M. D. King, Y.-X. Hu, and S. T. Bedka (2005b), Bulk scattering properties for the remote sensing of ice clouds, Part II: Narrowband Models. *J. Appl. Meteorol.*, 44, 1896–1911.
- Baum, B. A., P. Yang, S. Nasiri, A. K. Heidinger, A. J. Heymsfield, and J. Li (2007), Bulk Scattering Properties for the Remote Sensing of Ice Clouds. Part III: High resolution spectral models from 100 to 3250  $\text{cm}^{-1}$ . *J. Appl. Meteor. Clim.* 46, 423–434.
- Bohren, C. F., and D. R. Huffman (1983), *Absorption and scattering of light by small particles*. 530 pp., Wiley.
- Chylek, P., and J. Hallett (1992), Enhanced absorption of solar radiation by cloud droplets containing soot particles in their surface. *Q. J. R. Meteor. Soc.*, 118, 167–172.
- Chylek, P., G. B. Lesins, G. Videen, J. G. D. Wong, R. G. Pinnick, D. Ngo, and J. D. Klett (1996), Black carbon and absorption of solar radiation by clouds. *J. Geophys. Res.*, 101, 23,365–23,372.
- Chylek, P., V. Ramaswamy, and R.J. Cheng (1984), Effect of graphitic carbon on the albedo of clouds. *J. Atmos. Sci.*, 41, 3076–3084.
- Chylek P., G. Videen, D. J. W. Geldart, J. S. Dobbie, H. C. W. Tso (2000), Effective medium approximations for heterogeneous particles. In: Mishchenko M. I., J. W.

- Hovenier, L. D. Travis, editors. *Light scattering by nonspherical particles: theory, measurements, and applications*. San Diego: Academic Press, 273–308.
- Chylek, P., G. Videen, D. Ngo, R. G. Pinnick, and J. D. Klett (1995), Effect of black carbon on the optical properties and climate forcing of sulfate aerosols. *J. Geophys. Res.*, *100*, 16,325–16,332.
- Clarke, A. D., et al. (2004), Size distributions and mixtures of dust and black carbon aerosol in Asian outflow: Physiochemistry and optical properties. *J. Geophys. Res.*, *109*, D15S09, doi:10.1029/2003JD004378.
- Danielson, R., D. Moore, and H. van de Hulst (1969), The transfer of visible radiation through clouds. *J. Atmos. Sci.*, *26*, 1078–1087.
- Davis, C., C. Emde, and R. Harwood (2005), A 3-D polarized reversed Monte Carlo radiative transfer model for millimeter and submillimeter passive remote sensing in cloudy atmospheres. *IEEE Trans. Geosci. Remote Sens.*, *43*, 1096–1101.
- de Haan, J. F., P. B. Bosma, and J. W. Hovenier (1987), The adding method for multiple scattering calculations of polarized light. *Astron. Astrophys.*, *183*, 371–391.
- Evans, K. F., and G. L. Stephens (1991), A new polarized atmospheric radiative transfer model. *J. Quant. Spectrosc. Radiat. Transfer*, *46*, 413–423.
- Foot, J. S. (1988), Some observations of the optical properties of clouds. Part II: Cirrus. *Q. J. R. Meteorol. Soc.*, *114*, 145–164.
- Fuller, K. A. (1993), Scattering of light by coated spheres. *Opt. Lett.*, *18*, 257–259.
- Fuller, K. A., and D. W. Mackowski (2000), Electromagnetic scattering by compounded spherical particles. In: Mishchenko M. I., J. W. Hovenier, L. D. Travis, editors.



- Light scattering by nonspherical particles: theory, measurements, and applications*. San Diego: Academic Press, 225–272.
- Gao, B.-C., K. Meyer, and P. Yang (2004), A new concept on remote sensing of cirrus optical depth and effective ice particle size using strong water vapor absorption channels near 1.38 and 1.88  $\mu\text{m}$ . *IEEE Trans. Geosci. Remote Sens.*, *42*, 1891–1899.
- Gayet, J.-F., G. Fevre, G. Brogniez, H. Chepfer, W. Renger, and P. Wendling, 1996: Microphysical and optical properties of cirrus and contrails: Cloud field study on 13 October 1989. *J. Atmos. Sci.*, *53*, 126–138.
- Gierens, K. M., and J. Ström (1998), A numerical study of aircraft wake induced ice cloud formation. *J. Atmos. Sci.*, *55*, 3253–3263.
- Gothe, M. B., and H. Grassl (1993), Satellite remote sensing of the optical depth and mean crystal size of thin cirrus and contrails. *Theor. Appl. Climatol.*, *48*, 101–113.
- Hansen, J. E., and L. D. Travis (1974), Light scattering in planetary atmospheres. *Space Science Rev.*, *16*, 527–610.
- Hong, G. (2007), Parameterization of scattering and absorption properties of nonspherical ice crystals at microwave frequencies. *J. Geophys. Res.*, *112*, D11208, doi:10.1029/2006JD008364.
- IPCC (1999), *Special report on aviation and the global atmosphere*, edited by: Penner, J. E., Lister, D. H., Griggs, D. J., Dokken, D. J., and McFarland, M., Intergovernmental Panel on Climate Change, Cambridge University Press, New York, NY, USA.

- Kaiser, T., and G. Schweiger (1993), Stable algorithm for the computation of Mie coefficients for scattered and transmitted fields of a coated sphere. *Comput. Phys.*, 1993, 7, 682–686.
- Kärcher, B., O. Möhler, P. J. DeMott, S. Pechtl, and F. Yu (2007), Atmospheric Chemistry and Physics Insights into the role of soot aerosols in cirrus cloud formation. *Atmos. Chem. Phys.*, 7, 4203–4227.
- Kattawar, G. W., and D. A. Hood (1976), Electromagnetic scattering from a spherical polydispersion of coated spheres. *Appl. Opt.*, 15, 1996–1999.
- Kattawar, G. W., and G. N. Plass (1968), Radiance and polarization of multiple scattered light from haze and clouds. *Appl. Opt.*, 7, 1519–1527.
- King, M. D., S. Platnick, P. Yang, G. T. Arnold, M. A. Gray, J. C. Riédi, S. A. Ackerman, and K. N. Liou (2004), Remote sensing of liquid water and ice cloud optical thickness, and effective radius in the arctic: Application of airborne multispectral MAS data. *J. Atmos. Ocean. Technol.*, 21, 857–875.
- Kokhanovsky, A. A., (Ed.) (2006), *Light scattering reviews: Single and multiple light scattering*, 493 pp., Springer, New York.
- Kuhn, M., A. Petzold, D. Baumgardner, and F. Schröder (1998), Particle composition of a young condensation trail and of upper tropospheric aerosol. *Geophys. Res. Lett.*, 25, 2679–2682.
- Levoni, C., M. Cervino, R. Guzzi, and F. Torricella (1997), Atmospheric aerosol optical properties: A database of radiative characteristics for different components and classes. *Appl. Opt.*, 36, 8031–8041.

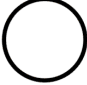
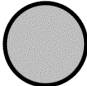

- Liu, L., and M. I. Mishchenko (2005), Effects of aggregation on scattering and radiative properties of soot aerosols. *J. Geophys. Res.*, *110*, D11211, doi:10.1029/2004JD005649.
- Liu, L., and M.I. Mishchenko (2007), Scattering and radiative properties of complex soot and soot-containing aggregate particles. *J. Quant. Spectrosc. Radiat. Transfer*, *106*, 262–273.
- Liu, L., M. I. Mishchenko, S. Menon, A. Macke, and A. A. Lacis (2002), The effect of black carbon on scattering and absorption of solar radiation by cloud droplets. *J. Quant. Spectrosc. Radiat. Transfer*, *74*, 195–204.
- Macke, A. (2000), Monte Carlo calculations of light scattering by large particles with multiple internal inclusions. In: Mishchenko M. I., J. W. Hovenier, L. D. Travis, editors. *Light scattering by nonspherical particles: theory, measurements, and applications*. San Diego: Academic Press, 309–322.
- Mackowski, D. W. (2006), A simplified model to predict the effects of aggregation on the absorption properties of soot particles. *J. Quant. Spectrosc. Radiat. Transfer*, *100*, 237–249.
- Meerkötter, R., U. Schumann, D. R. Doelling, P. Minnis, T. Nakajima, and Y. Tsushima (1999), Radiative forcing by contrails. *Ann. Geophys.*, *17*, 1070–1084.
- Minnis, P., J. K. Ayers, R. Palikonda, D. Phan (2004), Contrails, Cirrus Trends, and Climate. *J. Climate*, *17*, 1671–1685.
- Minnis, P., R. Palikonda, B. J. Walter, J. K. Ayers, and H. Mannstein (2005), Contrail properties over the eastern North Pacific from AVHRR data. *Meteorol. Z.*, *14*, 515–523.

- Minnis, P., U. Schumann, D. R. Doelling, K. Gierens, and D. Fahey (1999), Global distribution of contrail radiative forcing. *Geophys. Res. Lett.*, *26*, 1853–1856.
- Minnis, P., D. F. Young, D. P. Garber, L. Nguyen, W. L. Smith Jr., and R. Palikonda (1998), Transformation of contrails into cirrus during SUCCESS. *Geophys. Res. Lett.*, *25*, 1157–1160.
- Mishchenko, M. I., J. W. Hovenier, and L. D. Travis (2000), *Light Scattering by Nonspherical Particles: Theory, Measurements, and Applications*, Academic Press, San Diego.
- Mishchenko, M.I., L. Liu, L.D. Travis, and A.A. Lacis (2004), Scattering and radiative properties of semi-external versus external mixtures of different aerosol types. *J. Quant. Spectrosc. Radiat. Transfer*, *88*, 139–147.
- Myhre, G., and F. Stordal (2001), Global sensitivity experiments of the radiative forcing due to mineral aerosols. *J. Geophys. Res.*, *106*, 18,193–18,204.
- Parol, F., J. C. Buriez, G. Brogniez, and Y. Fouquart (1991), Information content of AVHRR channels 4 and 5 with respect to the effective radius of cirrus cloud particles. *J. Appl. Meteor.*, *24*, 973–984.
- Petzold, A., et al. (1997), Near field measurements on contrail properties from fuels with different sulfur content. *J. Geophys. Res.*, *102*, 29,867–29,880.
- Ponater, M., S. Marquart, and R. Sausen (2002), Contrails in a comprehensive global climate model: Parameterisation and radiative forcing results. *J. Geophys. Res.*, *107*, 10.1029/2001JD000429.
- Pruppacher, H. R., and J. D. Klett (1980), *Microphysics of clouds and precipitation*, 714 pp., Springer, New York.

- Schörder, F.; B. Kärcher, C. Duroure, J. Ström, A. Petzold, J.-F. Gayet, B. Strauss, P. Wendling, S. Borrmann (2000), On the transition of contrails into cirrus clouds. *J. Atmos. Sci.*, 57, 464–480.
- Schulz, F. M., K. Stamnes, and F. Weng (1999), VDISORT: An improved and generalized discrete ordinate method for polarized (vector) radiative transfer. *J. Quant. Spectrosc. Radiat. Transfer*, 61, 105–122.
- Ström J., and S. Ohlsson (1998), In situ measurements of enhanced crystal number densities in cirrus clouds caused by aircraft exhaust. *J. Geophys. Res.* 103, 11,355–11,361.
- Stuber, N., and P. M. Forster (2007), The impact of diurnal variations of air traffic on contrail radiative forcing. *Atmos. Chem. Phys.*, 7, 3153–3162.
- Toon, O. B., and T. P. Ackerman (1981), Algorithms for the calculation of scattering by stratified spheres. *Appl. Opt.*, 20, 3657–3660.
- Twohy, C. H., A. D. Clarke, S. G. Warren, L. F. Radke, R. J. Charlson (1989), Light-absorbing material extracted from cloud droplets and its effect on cloud albedo. *J. Geophys. Res.*, 94, 8623–8631.
- Van de Hulst, H. C. (1957), *Light Scattering by Small Particles*, 470 pp., Dover, Mineola, New York.
- Vermote, E. F., D. Tanre, J. L. Deuze, M. Herman, and J. J. Morcrette (1997), Second simulation of the satellite signal in the solar spectrum, 6S: An overview. *IEEE Trans. Geosci. Remote Sens.*, 35, 675–686.
- Warren, S. G. (1984), Optical constants of ice from ultraviolet to the microwave. *Appl. Opt.*, 23, 1206–1225.

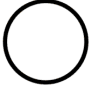



- Weng, F. (1992a), A multi-layer discrete-ordinate method for vector radiative transfer in a vertically-inhomogeneous, emitting and scattering atmosphere I: Theory. *J. Quant. Spectrosc. Radiat. Transfer*, 47, 19–33.
- Weng, F. (1992b), A multi-layer discrete-ordinate method for vector radiative transfer in a vertically-inhomogeneous, emitting and scattering atmosphere II: Application. *J. Quant. Spectrosc. Radiat. Transfer*, 47, 35–42.
- Yang, P., et al. (2002), Inherent and apparent scattering properties of coated or uncoated spheres embedded in an absorbing host medium. *Appl. Opt.* 41, 2740–2759.
- Yang, P., K. N. Liou, K. Wyser, and D. Mitchell (2000), Parameterization of the scattering and absorption properties of individual ice crystals. *J. Geophys. Res.*, 105, 4699–4718.
- Yang, P., H. Wei, H.-L. Huang, B. A. Baum, Y. X. Hu, G. W. Kattawar, M. I. Mishchenko, and Q. Fu (2005), Scattering and absorption property database for nonspherical ice particles in the near- through far-infrared spectral region. *Appl. Opt.*, 44, 5512–5523.

Table 1. Refractive indexes of ice particles considered in the present study.

Ice Particle	Wavelength ( $\mu\text{m}$ )	Refractive Index
	0.65	$1.30804 + 1.4325\text{E-}08i$
	2.13	$1.26732 + 5.5682\text{E-}04i$
	0.65	$1.39643 + 0.08600i$
	2.13	$1.37490 + 0.09949i$
	0.65	$*1.75000 + 0.43000i$
	2.13	$*1.80520 + 0.49520i$

\* for black carbon in core or shell.

Table 2. Bulk scattering properties of ice particles in a young contrail with a  $D_e = 1.5 \mu\text{m}$ .

Ice Particles	Wavelength ( $\mu\text{m}$ )	Absorption Efficiency ( $\bar{Q}_{abs}$ )	Scattering Efficiency ( $\bar{Q}_{sca}$ )	Extinction Efficiency ( $\bar{Q}_{ext}$ )	Single- scattering Albedo ( $\bar{\omega}$ )	Asymmetry Factor ( $\bar{g}$ )
	0.65	3.39506e-07	3.305950	3.30595	1.000000	0.785125
	2.13	0.00433447	0.641332	0.64567	0.993287	0.684770
	0.65	1.128330	1.633380	2.76176	0.591438	0.880037
	2.13	0.624601	0.875466	1.50007	0.583618	0.694842
	0.65	0.745810	2.00990	2.75571	0.729358	0.766256
	2.13	0.603505	0.766096	1.36960	0.559357	0.597429
	0.65	0.896992	2.22333	3.12032	0.712532	0.843413
	2.13	0.590587	0.842937	1.43352	0.588017	0.693491



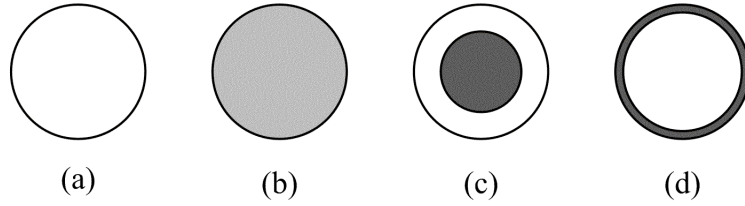


Figure 1. Four types of ice particles in young contrails used in the present study. (a) pure ice particle, (b) representing the internal mixture of ice and black carbon, (c) coated soot with ice, (d) coated ice with black carbon. The volume mixing ratio of black carbon in (b)–(d) is assumed to be 20% in the present study.

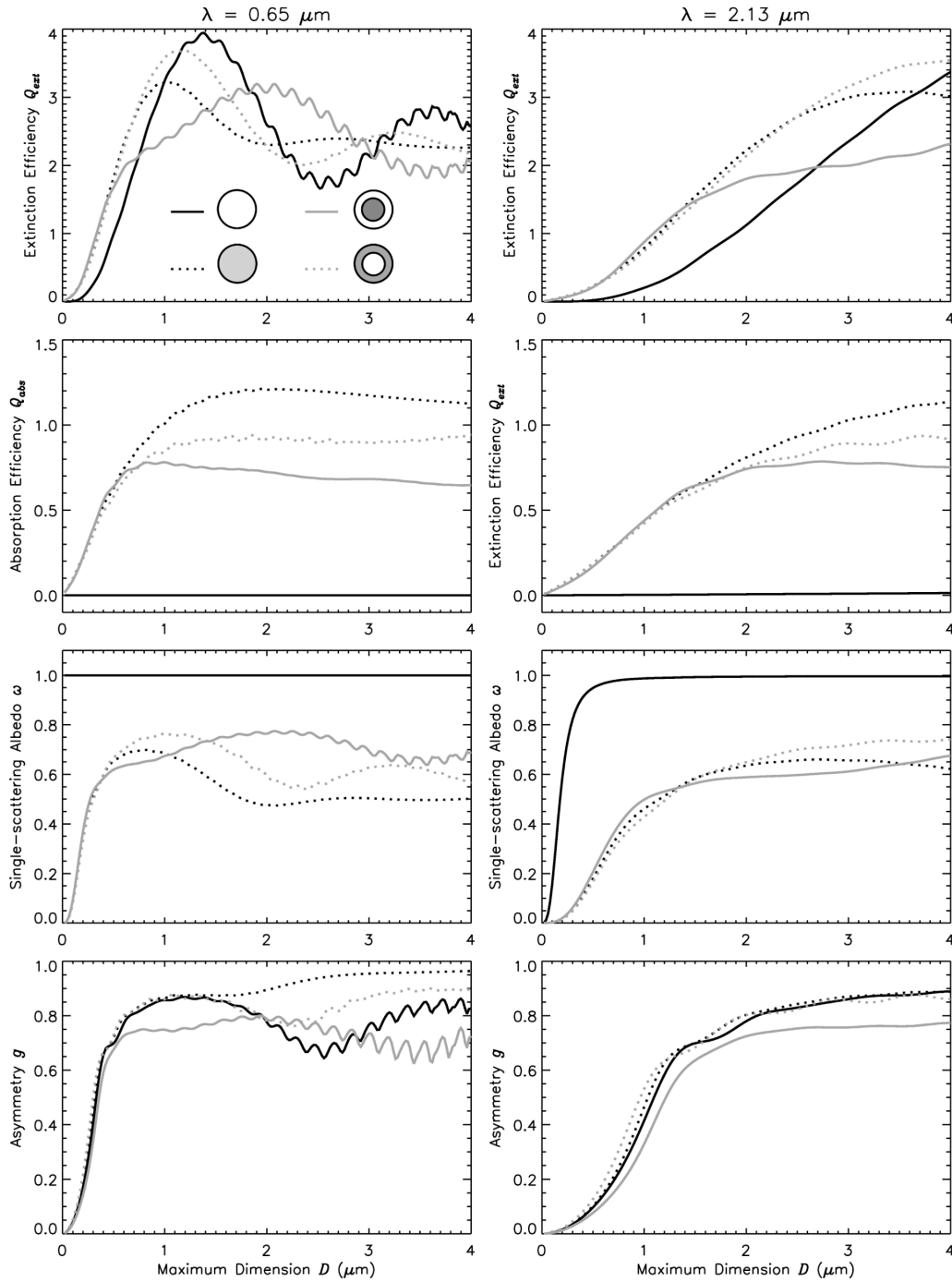


Figure 2. Single-scattering properties (extinction efficiency  $Q_{ext}$ , absorption efficiency  $Q_{abs}$ , single-scattering albedo  $\omega$ , and asymmetry factor  $g$ ) of ice particles in young contrails.

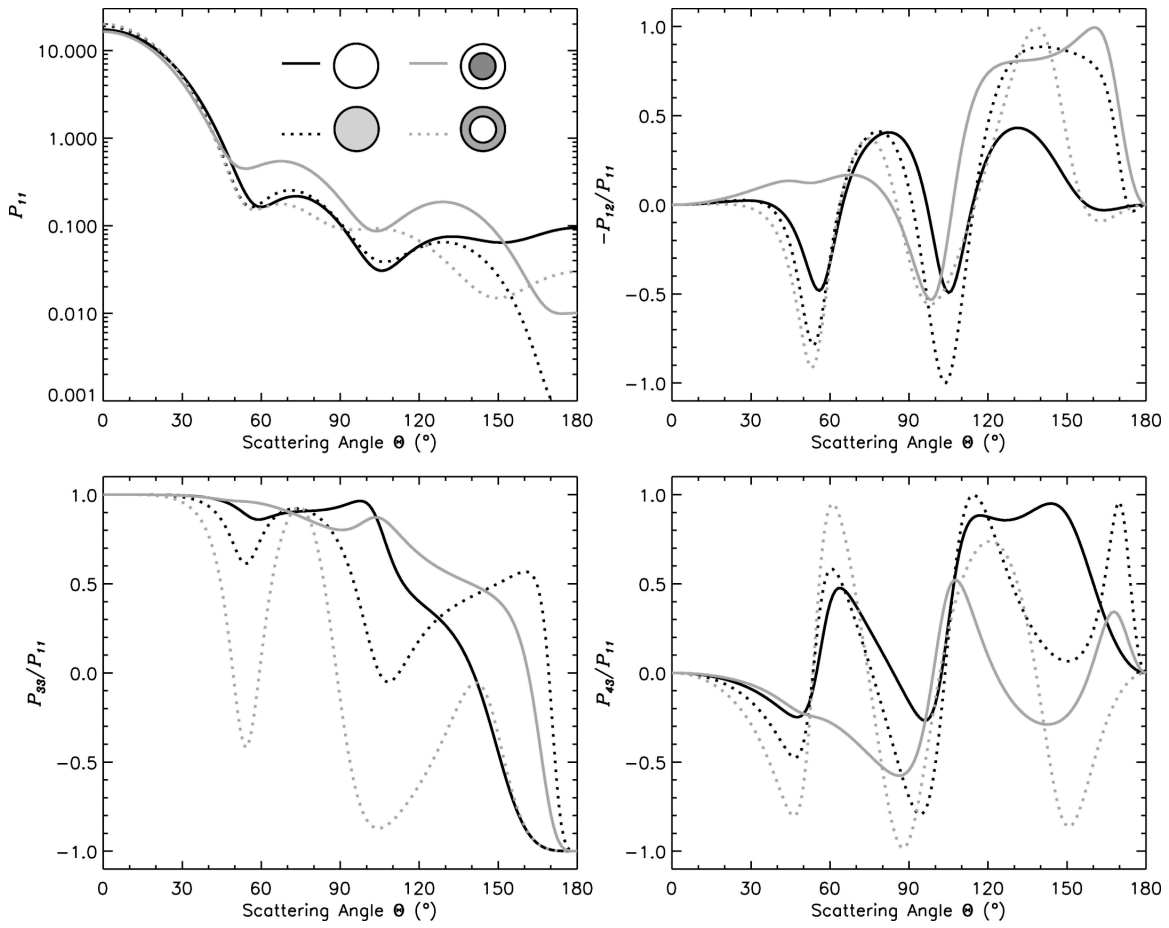


Figure 3. Phase matrix as a function of scattering angle at  $0.65 \mu\text{m}$  with a size parameter of 4.0 for ice particles in young contrails.

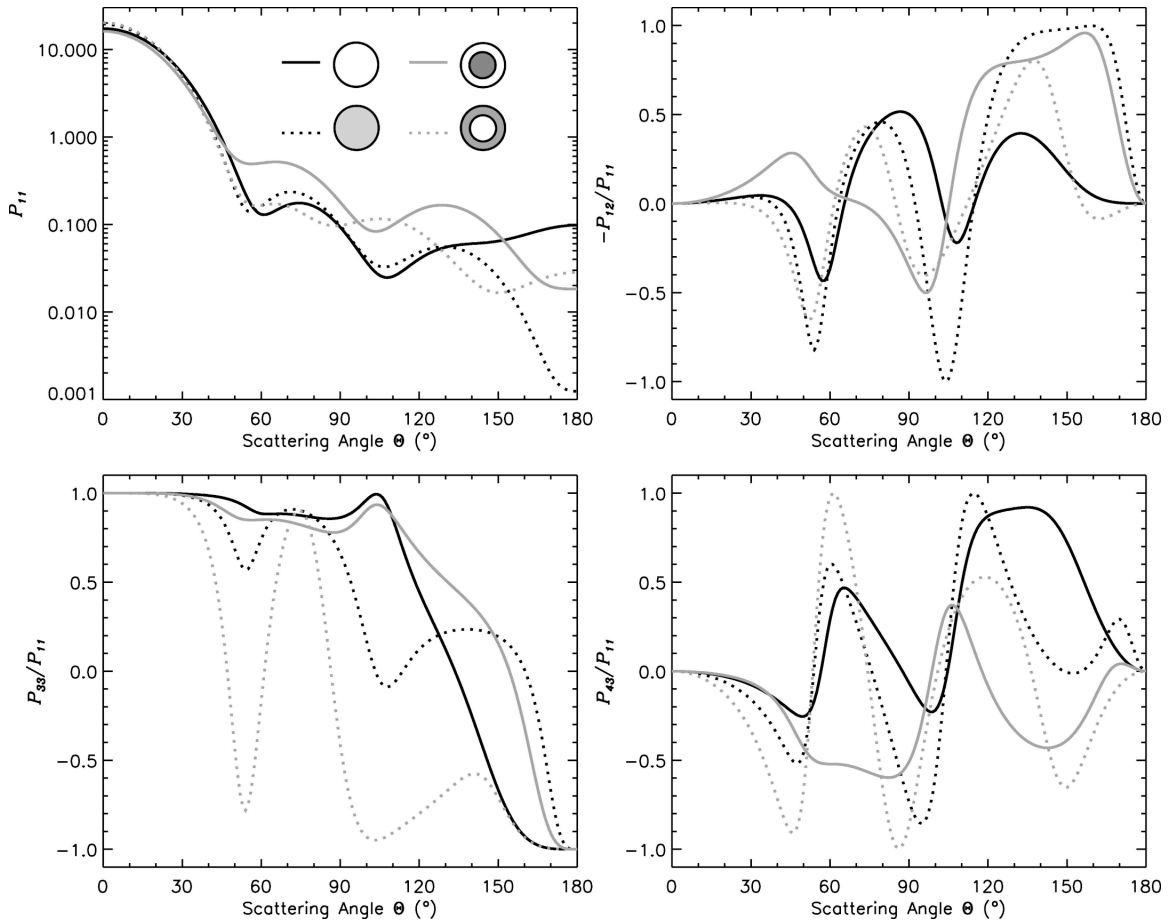


Figure 4. Same as Figure 3, but for 2.13  $\mu\text{m}$ .

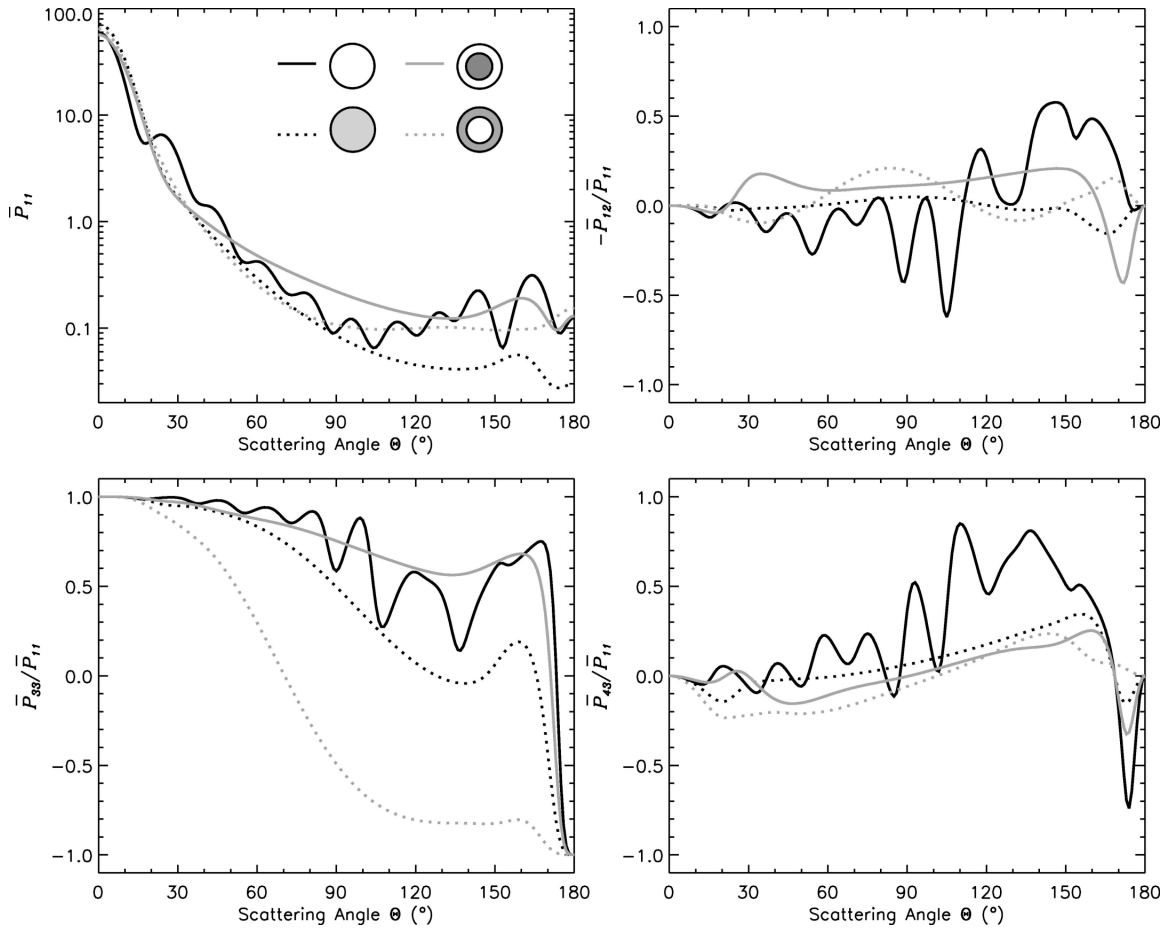


Figure 5. Mean phase matrix as a function of scattering angle at  $0.65 \mu\text{m}$  for a young contrail with an effective particle size of  $1.5 \mu\text{m}$ .

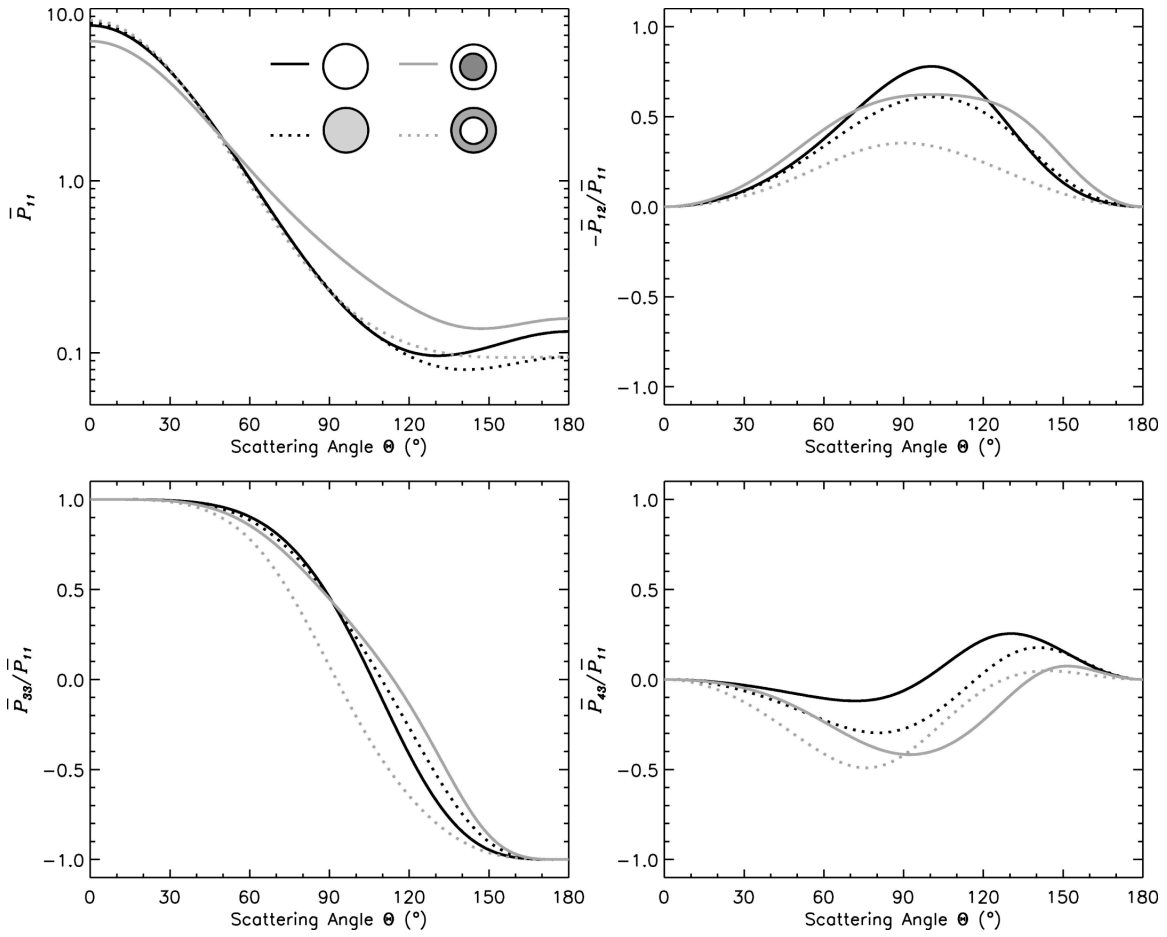


Figure 6. Same as Figure 5, but for  $2.13 \mu\text{m}$ .

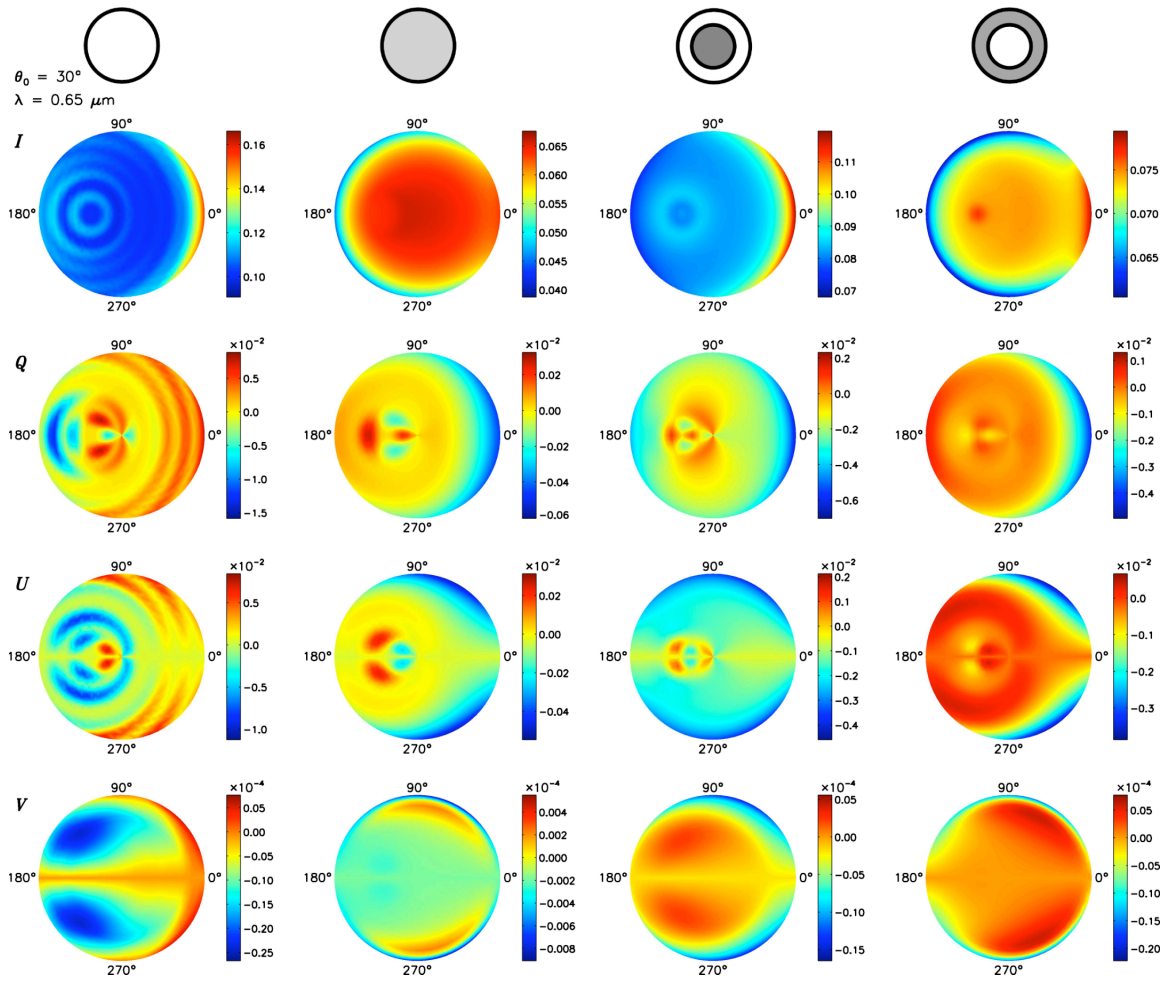


Figure 7. Simulated Stokes parameters ( $I$ ,  $Q$ ,  $U$ ,  $V$ ) by young contrails composed of the four types of ice crystals considered in the present study for the wavelength  $0.65 \mu\text{m}$ .

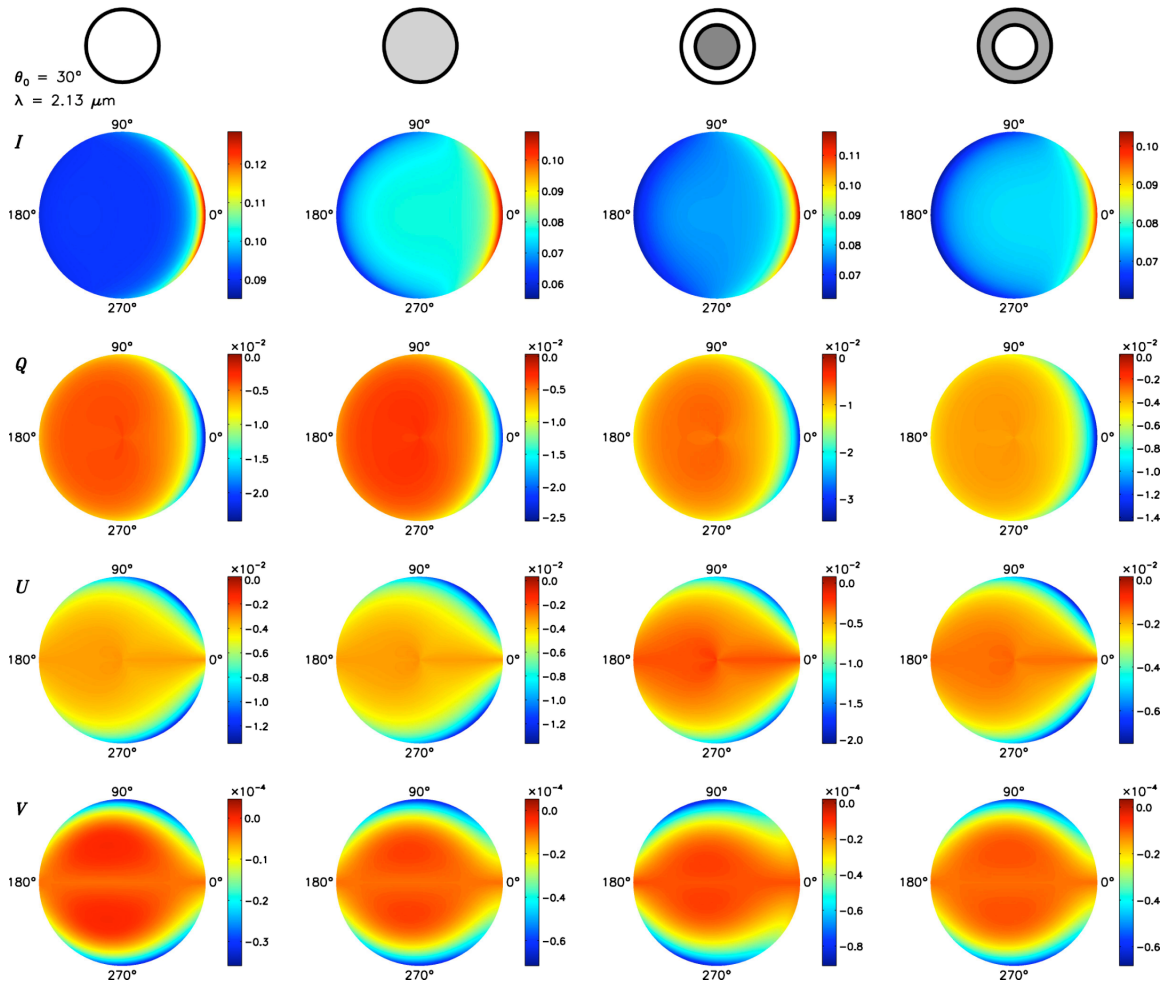


Figure 8. Same as Figure 7 but for  $2.13 \mu\text{m}$ .